

ISTS-2006-160645

THE SPACE TECHNOLOGY-7 DISTURBANCE REDUCTION SYSTEM PRECISION CONTROL FLIGHT VALIDATION EXPERIMENT CONTROL SYSTEM DESIGN

James R. O'Donnell, Ph.D., Oscar C. Hsu, Peiman G. Maghami, Ph.D., F. Landis Markley, Ph.D.

NASA Goddard Space Flight Center

Mission Engineering and Systems Analysis Division, Code 590

Greenbelt, Maryland 20771 USA

James.R.ODonnell@nasa.gov

Abstract

As originally proposed, the Space Technology-7 Disturbance Reduction System (DRS) project, managed out of the Jet Propulsion Laboratory, was designed to validate technologies required for future missions such as the Laser Interferometer Space Antenna (LISA). The two technologies to be demonstrated by DRS were Gravitational Reference Sensors (GRSs) and Colloidal MicroNewton Thrusters (CMNTs). Control algorithms being designed by the Dynamic Control System (DCS) team at the Goddard Space Flight Center would control the spacecraft so that it flew about a freely-floating GRS test mass, keeping it centered within its housing.

For programmatic reasons, the GRSs were descope from DRS. The primary goals of the new mission are to validate the performance of the CMNTs and to demonstrate precise spacecraft position control. DRS will fly as a part of the European Space Agency (ESA) LISA Pathfinder (LPF) spacecraft along with a similar ESA experiment, the LISA Technology Package (LTP). With no GRS, the DCS attitude and drag-free control systems make use of the sensor being developed by ESA as a part of the LTP. The control system is designed to maintain the spacecraft's position with respect to the test mass, to within $10 \text{ nm}/\sqrt{\text{Hz}}$ over the DRS science frequency band of 1 to 30 mHz.

1. Introduction and Overview

The Space Technology-7 mission is a Disturbance Reduction System (DRS) flight validation experiment within NASA's New Millennium Program [1]. New Millennium Program missions are intended to validate advanced technologies that have not flown in space in order to reduce the risk of their infusion into future NASA science missions. DRS originally incorporated two new technologies, a highly sensitive Gravitational Reference Sensor (GRS) to measure the position and attitude of a spacecraft with respect to an internal free-floating test mass, and a set of Colloidal MicroNewton Thrusters (CMNTs) to provide low-noise control of the spacecraft for drag-free flight. The GRS was recently descope, leaving the CMNTs as the sole new technology being demonstrated by DRS. The system is scheduled to fly on the European Space Agency's (ESA) LISA

Pathfinder (LPF) spacecraft in 2009, (LISA Pathfinder is an ESA mission funded by the ESA member states and NASA) and will operate in an orbit about the Earth-Sun L1 point. With the descope of the GRS, DRS will now close its control loop using the output of the European inertial sensor, which is part of the LISA Technology Package (LTP), also flying on LPF. This sensor is referred to as the Drag-Free Sensor (DFS).

Fig. 1 shows a schematic of the elements of the DRS. The DRS is designed to maintain the spacecraft's position, with respect to the free-floating test mass, to less than $10 \text{ nm}/\sqrt{\text{Hz}}$, over DRS's science band, a frequency range from 1 to 30 mHz. This requirement will help ensure that the residual accelerations on the GRS test masses (beyond gravitational acceleration) will be below $3 \times 10^{-14} [1 + (f/3 \text{ mHz})^2] \text{ m/s}^2/\sqrt{\text{Hz}}$, the DRS goal. The DRS instrument package consists of two sets of four Colloidal MicroNewton Thrusters (CMNTs) each for position and attitude control, and an Integrated Avionics Unit (IAU) that hosts the software implementing the Dynamic Control System (DCS) control algorithms.

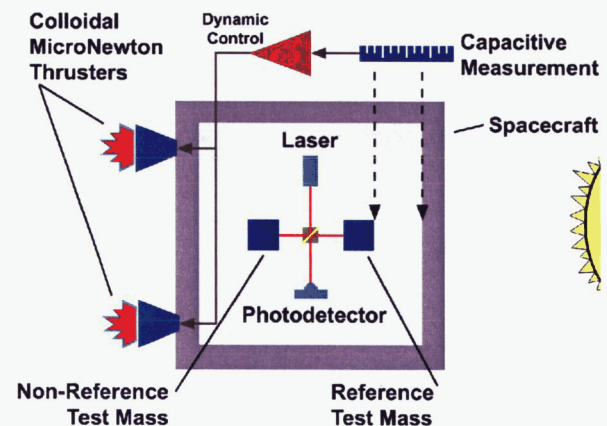


Figure 1: DRS Schematic

The goal of the DCS, when in drag-free operation, is to use small thrusters to fly a spacecraft about a test mass such that the test mass follows a purely gravitational trajectory, unaffected by the spacecraft or any external disturbances to some tolerance. The performance measure for a gravitational reference sensor is the residual acceleration in the frequency band of interest (dictated by the mission). These residual accelerations come from

sources such as time varying temperatures, residual gas pressure, magnetic forces acting on the test mass, internal gravity between the test mass and the spacecraft, and cross-talk from the electrostatic suspension control of the Drag Free Sensor (DFS).

The first drag-free mission, known as TRIAD-1, was flown in 1973 [2]. The DRS goal at the time of its inception was to demonstrate a level of residual acceleration more than four orders of magnitude lower than previously demonstrated in space [3]. With the launch and successful operation of GRACE, the DRS goal is closer to three orders of magnitude better.

A high level overview of DRS is given in [4], and the CMNTs are described in [5]. The purpose of this paper is to give an overview of the new elements of the DCS; with the descope of the GRS, the DCS team was given the responsibility for designing the test mass control systems in addition to those for the spacecraft. Design information and simulation results will be given for the DCS control modes that rely on only one test mass. The two-test mass control modes will be described at a later date.

2. Control Strategy & DRS Mission Modes

Table 1 shows a description of the DRS Mission Modes being implemented to carry out the various operations needed on the spacecraft. The modes are shown in the order they will be used to gradually shift from simple attitude control of the spacecraft to full 18 degree-of-freedom position and attitude control of the spacecraft and both test masses. For each DRS Mission Mode, there is a corresponding combination of spacecraft control mode and control modes for the two test masses, denoted the Reference Test Mass (RTM) and Non-Reference Test Mass (NTM). In addition to the test mass control mode, each test mass can be controlled in what is known as High Force or Low Force. High Force has greater control authority and correspondingly higher actuation noise, while Low Force has less control authority but much better noise characteristics. In Table 1, the test mass control modes that use Low Force are shaded and shown with an asterisk (*).

A short description and the purpose of each DRS Mission Mode is as follows:

- **Attitude Control:** The main purpose of this mode is to perform initial capture of the spacecraft when control is handed over from LPF. The spacecraft is controlled in attitude only, while both test masses are controlled in accelerometer mode, where the electrostatic suspension system is commanded to center them in their housings.
- **Zero-G:** This is the mode in which the spacecraft first tries to counteract external forces, primarily the solar radiation pressure force. Test mass control is the same accelerometer control used in the previous mode. However, while controlling the spacecraft's orientation, the spacecraft's position is controlled in order to minimize the force commands applied to the reference test mass. The spacecraft position control (drag-free controller) uses the suspension forces generated by the RTM's suspension control as a measure of spacecraft acceleration.
- **Drag-Free/High Force & Drag-Free/Low Force:** The Drag-Free/Low Force mode is the one in which the spacecraft flies drag-free about the RTM within the DRS requirements. The 10 nm/ $\sqrt{\text{Hz}}$ performance requirement in the science band can be demonstrated in this mode. The High Force version of this mode is used as a transition step to get into Low Force.
- **18-DOF/Transitional & 18-DOF:** In 18-DOF, the spacecraft flies drag-free about the RTM while also flying drag-free within the science band in the transverse axes about the NTM, and the roll axis of the RTM. The second test mass is needed to measure the acceleration performance of the controller, and the LTP includes an interferometer to measure the relative position and orientation of the two test masses. Because the DRS does not have its own drag-free sensor, the acceleration performance is treated as a goal and not a requirement.

This paper will discuss and give results for Attitude Control through Drag-Free/Low Force Modes. The 18-DOF modes and mode transition strategy will be discussed in a future publication.

Table 1: DRS Mission Modes

DRS Mission Mode	Spacecraft Mode	RTM Mode	NTM Mode
Attitude Control	Attitude-Only (AO)	DFS Accelerometer	DFS Accelerometer
Zero-G	Accelerometer (AC)	DFS Accelerometer	DFS Accelerometer
Drag-Free/High Force	Initial Drag-Free (DF1)	DFS Drag-Free 1	DFS Accelerometer
Drag-Free/Low Force	Initial Drag-Free (DF1)	DFS Drag-Free 1*	DFS Accelerometer
18-DOF/Transitional	Initial Drag-Free (DF1)	DFS Drag-Free 1*	DFS Suspended Drag-Free 1*
18-DOF	Science (SM)	DFS Drag-Free 2*	DFS Suspended Drag-Free 2*

2.1 Attitude Control Mode

The block diagram of Attitude Control Mode is depicted in Figure 2 and Figure 3. In this mode, the three control modes—for the spacecraft, for the RTM, and for the NTM—are decoupled from one another. The spacecraft controller controls its attitude based solely on the star tracker and target quaternions provided by LPF.

Body frame torque commands are converted using simple thruster distribution logic into force commands to the eight CMNTs. The spacecraft control system is designed to be low bandwidth so that star tracker noise will not dominate in the higher frequencies, and to keep the required thrust commands within the limited range of the CMNTs, while high enough to meet the requirements on spacecraft pointing and rates for handover and normal operations. The control design is a single-input single-output controller with each loop made up of a PID controller and a 4th order attenuation filter.

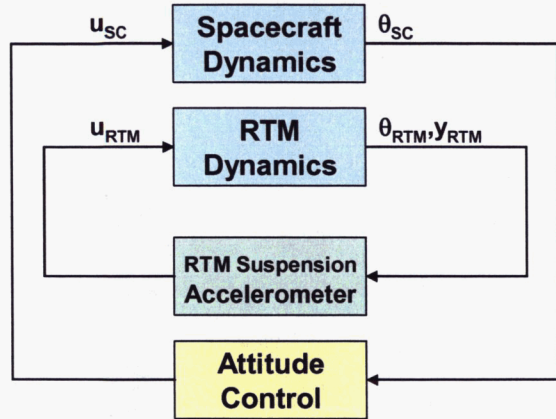


Figure 2: Attitude Control Mode Block Diagram

Both the RTM and NTM are controlled in translation and rotation via electrostatic suspension. The suspension control is designed to be high enough bandwidth so that each test mass follows its housing throughout and beyond the science band of 1–30 mHz. By measuring the applied force and torque commands while executing this control, each test mass becomes, in effect, an accelerometer. Note that the RTM and NTM control block diagrams are shown separately in Figure 2 and Figure 3, but in this mode the control for each is identical. In fact, the NTM control shown is the same in each Mission Mode from Attitude Control through Drag-Free/Low Force.

2.2 Zero-G Mode

The test mass control systems used for both the RTM and NTM in Zero-G Mode are identical to those used in Attitude Control Mode. The difference in this mode is that the force commands being sent to the RTM are also used to close a drag-free control loop for the spacecraft, as shown in the block diagram shown in Figure 4.

The attitude control loop shown in Figure 4 is identical to that of Attitude Control Mode. The difference is the addition of a drag-free control loop. The main

objective of this loop is to reduce the steady-state accelerations on the RTM by minimizing the applied suspension force command. The bandwidth of this controller is significantly larger than the attitude control loop to provide adequate disturbance rejection in the science band from the thruster force noise. Because of the high bandwidth, there is no adverse coupling with the attitude control loop.

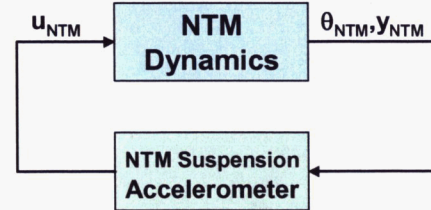


Figure 3: Non-Reference Test Mass Control

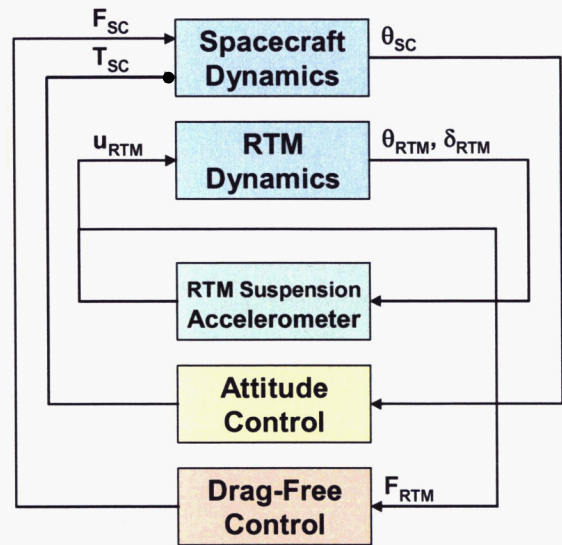


Figure 4: Zero-G Mode Block Diagram

2.3 Drag-Free Modes

The two Drag-Free Modes are the first in which the spacecraft flies drag-free, about one of the two test masses, the RTM. The block diagram for this mode is shown in Figure 5. The block diagram for this mode looks very similar to that of Zero-G Mode, and the attitude control loop is identical in each. There are two key differences.

Because the objective of this control mode is to fly the spacecraft drag-free about the RTM, the RTM control loop does not perform translational control. It is used only to issue torque commands to control the orientation of the RTM within its housing. Meanwhile, the spacecraft drag-free control loop takes as its input the gap errors output by the capacitive sensing of the LTP, and seeks to minimize those errors. Similar to the drag-free control loop in Zero-G Mode, the bandwidth of the controller is significantly larger than the attitude control loop to provide adequate disturbance rejection in the science

band from the thruster force noise and has no adverse coupling with the attitude control loop.

The drag-free control loop design is a SISO controller, which includes lead and lag compensators, integral action, and a 4th-order attenuation filter.

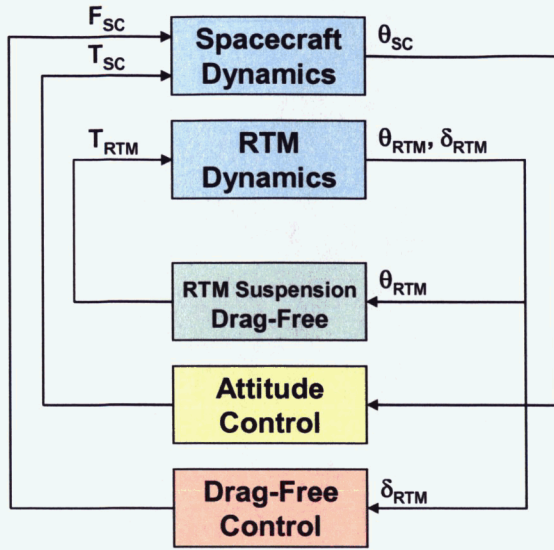


Figure 5: Drag-Free Mode Block Diagram

3. Simulation Results

In this section, simulation results from the three different DRS Mission Modes described in the previous section will be shown. An initial capture simulation will be shown for Attitude Control Mode, the ability of Zero-G Mode to compensate for solar radiation pressure force will be shown, and various plots showing drag-free operation on Drag-Free/Low Force Mode, including a power spectral density (PSD) plot verifying that the mode meets its design requirement, will be shown.

3.1 Initial Capture from LPF Control

The first use of Attitude Control Mode will be to capture the spacecraft after transition from LPF control. Initial spacecraft rates and attitude errors upon handover can be as high as 0.75° and 5 microradians/second (3σ). DRS is required to keep attitude errors and rates under 4° and 20 microradians/second for the first two hours after control handover, and 2° and 10 microradians/second thereafter.

An extensive worst-case initial capture analysis was done for Attitude Control Mode. First, capture performance analysis at all possible combinations of the worst-case values of 14 parameters was done (2048 cases). These included initial attitude offset, initial rates, external forces and torques, and spacecraft center of mass location. An additional 5000 simulations were performed using a Monte Carlo analysis over these same parameters. In each of these runs, it was assumed that a good initial estimate of the external force and torque environment was known—in flight, this will be supplied via LTP

data—and could be compensated for initially by the attitude control loop.

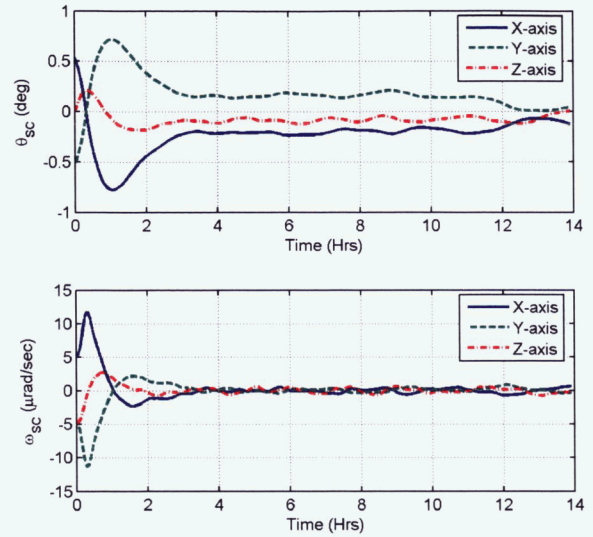


Figure 6: Initial Capture Attitude Errors & Rates

Figure 6 shows the spacecraft attitude errors and rates during a worst-case attitude excursion simulation. Note that the performance of the mode satisfies both maximum attitude excursion and rate requirements during the initial two hours and afterwards.

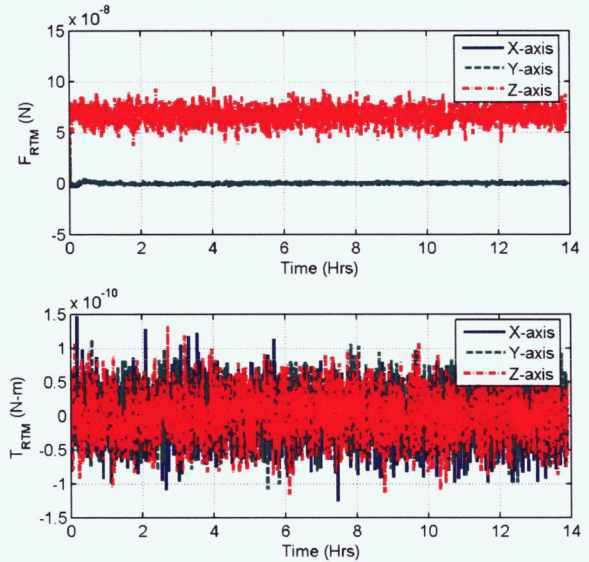


Figure 7: RTM Applied Forces & Torques

Figure 7 shows the control forces and torques applied to the RTM during this time. Remember that the spacecraft and test mass control are completely decoupled in Attitude Control Mode. This plot is shown for reference, so that the differences between this mode, Zero-G Mode, the Drag-Free Modes can be highlighted.

3.2 Solar Pressure Force Compensation

As mentioned previously, the most obvious feature of the DRS Zero-G Mode is that it is the first mode in which external forces acting on the spacecraft are compensated

for in a closed-loop fashion. Note that it is possible to compensate for them open-loop via the setting of appropriate thruster biases in Attitude Control Mode. The external forces acting on the spacecraft are dominated by the solar radiation pressure force, along with the force of the infrared re-radiation from the spacecraft that occurs as a result of solar heating.

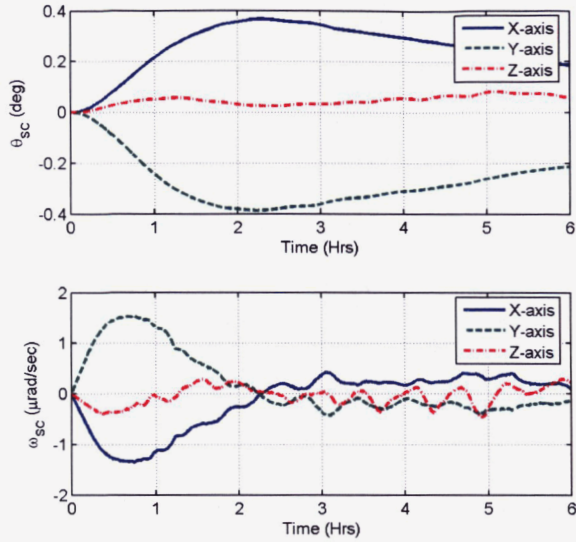


Figure 8: Attitude Errors & Rates in Zero-G Mode

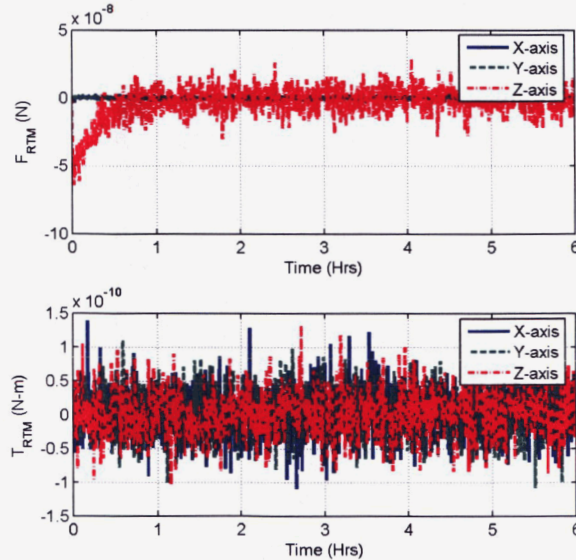


Figure 9: RTM Forces & Torques in Zero-G Mode

Figure 8 shows the spacecraft attitude errors and rates during six hours of a Zero-G Mode simulation. The controller easily meets its attitude error and rate requirements. Figure 9 shows the corresponding force and torque commands to the RTM. Note that the torque commands are very similar to that of the Attitude Control Mode controller seen in Figure 7, but that the Z-axis force commands are considerably lower magnitude. The Z-axis of the spacecraft corresponds to the sun direction; this shows that the Zero-G Mode is successfully using the

spacecraft to minimize the accelerations being applied to the test mass.

3.3 Drag-Free Operation

Figure 10 and Figure 11 show the spacecraft attitude errors and rates, and the applied force and torque for the RTM in Drag-Free/Low Force Mode. As expected, the spacecraft pointing error and rates meet their requirements. The first obvious feature of Figure 11 is that the applied force commands to the RTM are zero. Because the purpose of this mode is to fly the spacecraft drag-free about the RTM, no suspension forces are applied.

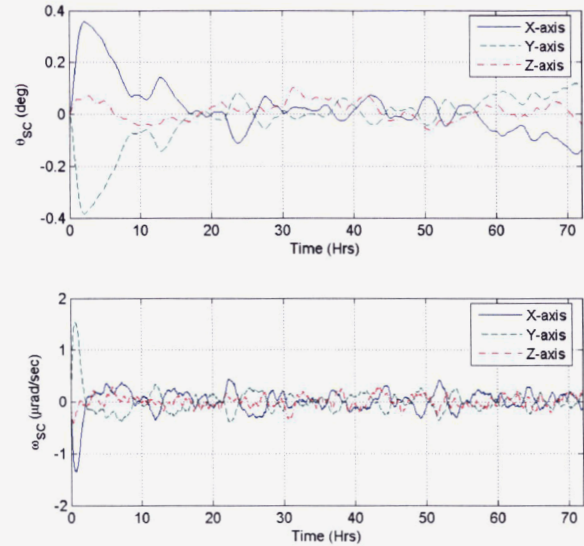


Figure 10: Attitude Performance While Drag-Free

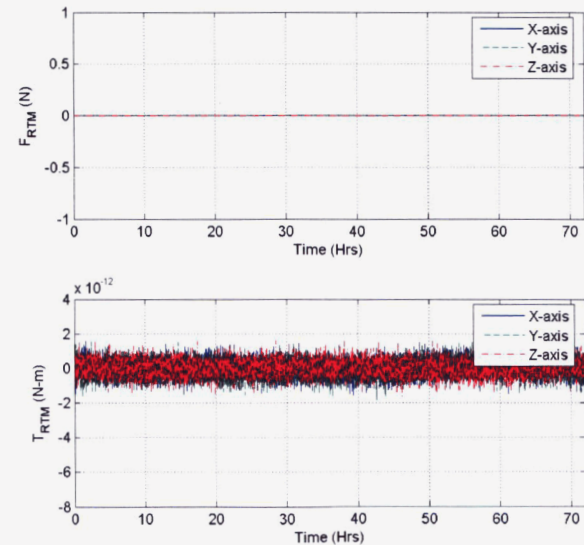


Figure 11: RTM Applied Torques While Drag-Free

Further, the applied torque commands are more than two orders of magnitude lower than those of Attitude Control and Zero-G Modes. While the test mass control performs the same function with respect to test mass attitude in all three modes, the substantially lower applied

torque commands are indicative of the much lower actuation noise of the drag-free sensor being used in its Low Force mode of operations. Also, the bandwidth of the suspension controller is substantially lower in this mode to enable its operation in the DFS Low Force mode.

In order to verify the primary requirement of the Drag-Free Mode, that the spacecraft follows the RTM such that the position error of the RTM with respect to its housing is better than $10 \text{ nm}/\sqrt{\text{Hz}}$ from 1 to 30 mHz, it is necessary to do a PSD of the time-domain results. A comparison of the results of the linear model and the high-fidelity (HiFi) simulation is shown in Figure 12. This figure shows that the design meets this requirement.

4. Conclusion

With the descope of its own gravitational reference sensor, the DRS project continued its mission by instead making use of the sensor being developed as a part of the LISA Technology Package. As a result of this change, the DCS team was required to redesign the existing spacecraft controllers, as well as design new test mass control systems. These designs have been completed and implemented and are currently undergoing flight software testing, as DRS continues to prepare for a September 2009 launch.

References

1. Keiser, G. M., et. al., "Disturbance Reduction System for Testing Technology for Drag-Free Operation," SPIE Paper 4856-02, Astronomical Telescopes and Instrumentation Conference, Waikoloa, Hawaii, USA, August 2002.
2. JHU-APL Space Department and Stanford University Guidance Control Laboratory, "A Satellite Freed of All but Gravitational Forces: TRIAD I," *AIAA Journal of Spacecraft*, Vol. 11, 637–644, 1974.
3. Folkner, W. M., et. al., *Disturbance Reduction System: A Concept Study Report for the New Millennium Program*, Jet Propulsion Laboratory, December, 2001.
4. Carmain, A., Dunn, C., Folkner, W., Hruby, V., Spence, D., O'Donnell, J., Markley, F., Maghami, P., and Hsu, O., "Space Technology 7 Disturbance Reduction System—Precision Control Flight Validation," IEEE Aerospace Conference, Big Sky, MT, USA, March 2005.
5. Hruby, V., Gamero-Castaño, M., Spence, D., Gasdaska, C., Demmons, N., McCormick, R., Falkos, P., Young, J., and Connolly, W., "Colloid Thrusters for the New Millennium, ST7 DRS Mission," IEEE Aerospace Conference, Big Sky, MT, USA, March 2004.
6. Maghami, P. G., Hsu, O. C., Markley, F. L., and O'Donnell, J.R., "Control Modes of the ST7 Disturbance Reduction System Flight Validation Experiment," SPIE Paper 5528A-17, International Symposium on Optical Science and Technology, Denver, Colorado, USA, August 2004.
7. Hsu, O. C., Maghami, P. G., Hsu, O. C., Markley, F. L., and O'Donnell, J.R., Jr., "Mode Transitions for the ST7 Disturbance Reduction System Experiment," AIAA Paper 2004-5429, AIAA Guidance, Navigation & Control Conference, Providence, Rhode Island, USA, August 2004.

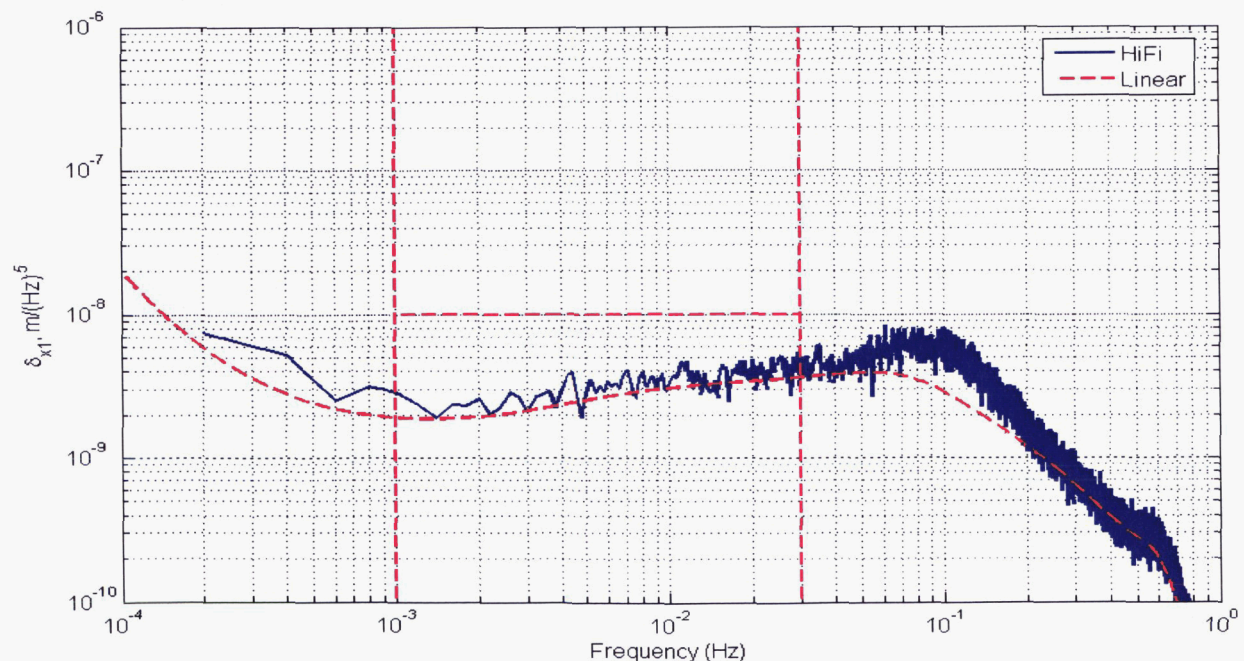


Figure 12: Reference Test Mass Drag-Free Position Performance PSD